Electronic Supplementary Material (ESI) for Inorganic Chemistry Frontiers.

Ultrafast synthesis of SAPO-17 zeolites with excellent CO_2/N_2 and CO_2/CH_4 separation performance

Chaoran Wang,[a] Xiao Li,[a] Shiyue Liu,[a] Tingting Wang,[a] Puxu Liu,[b] Xiaowei Song*[a], and Zhiqiang Liang*[a]

[a]*State Key Laboratory of Inorganic Synthesis and Preparative Chemistry, College of Chemistry, Jilin University, 2699 Qianjin Street, Changchun 130012, P. R. China*

[b]*College of Chemistry and Chemical Engineering, Shanxi Key Laboratory of Gas Energy Efficient and Clean Utilization, Taiyuan University of Technology, Taiyuan 030024, Shanxi, China*

*Corresponding Authors.

E-mail addresses: xiaoweisong@jlu.edu.cn (X. W. Song), liangzq@jlu.edu.cn (Z. Q. Liang).

Section 1 Calculation of Q_{st}

$$InP = InN + {}^{1}/_{T}\sum_{i=0}^{m} a_i N^i + \sum_{i=0}^{n} b_j N^j$$

$$Q_{st} = -R\sum_{i=0}^{m} a_i N^i$$

Where N represents the adsorption capacity (cm^3/g), P is the pressure (mmHg), T is the temperature (K), a_i and b_j are constants, and R is 8.314 J/mol/K.

Section 2 Langmuir Freundlich formula

$$q = q_{m_1}\frac{b_1 P^{\frac{1}{C_1}}}{1 + b_1 P^{\frac{1}{C_1}}} + q_{m_2}\frac{b_2 P^{\frac{1}{C_2}}}{1 + b_2 P^{\frac{1}{C_2}}}$$

Where p is the pressure of the gas when the adsorption reaches equilibrium (kPa); q is the adsorption capacity per unit mass of adsorbent (mol/kg), q_{m1} and q_{m2} are the saturated capacity of component 1 and component 2 (mol/kg), respectively; b_1 and b_2 represent the affinity coefficients of component 1 and component 2 (1/kPa); C_1 and C_2 are deviations from the ideal uniform surface.

Separation factor (S)

$$S = \frac{q_1/q_2}{P_1/P_2}$$

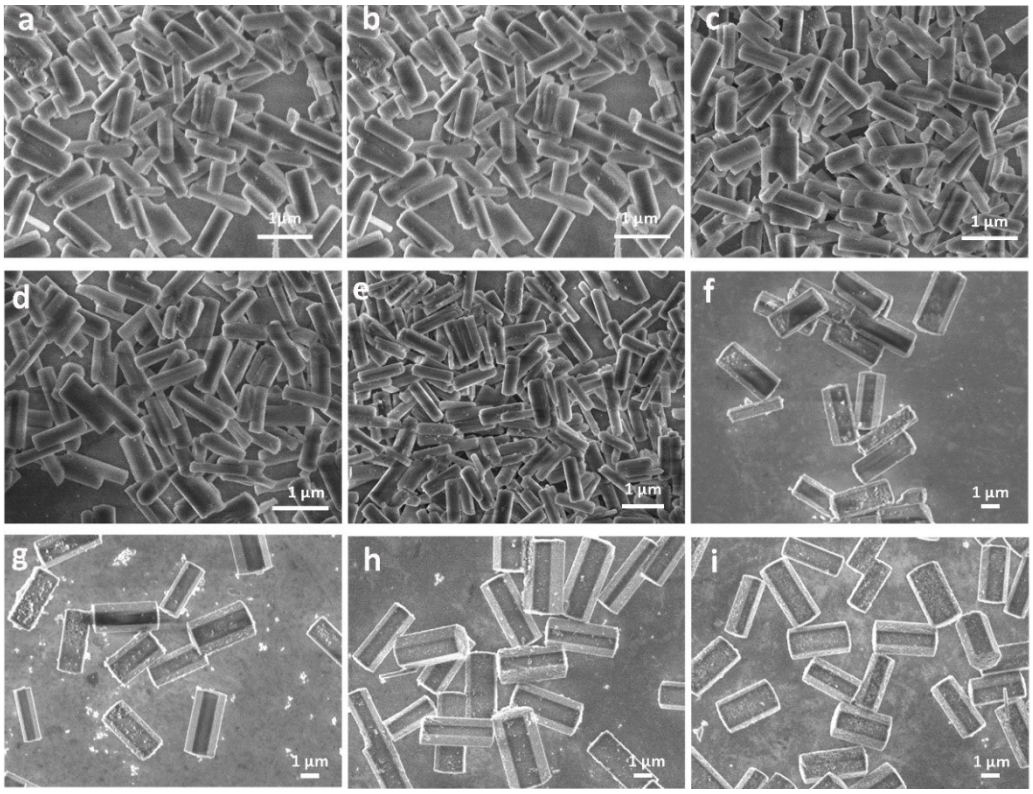

Fig. S1 Scanning electron microscopy (SEM) images of SAPO-17-S-3 (a), SAPO-17-S-5 (b), SAPO-17-S-10 (c), SAPO-17-S-15 (d), SAPO-17-S-30 (e), SAPO-17-S-60 (f), SAPO-17-S-120 (g), SAPO-17-S-180 (i).

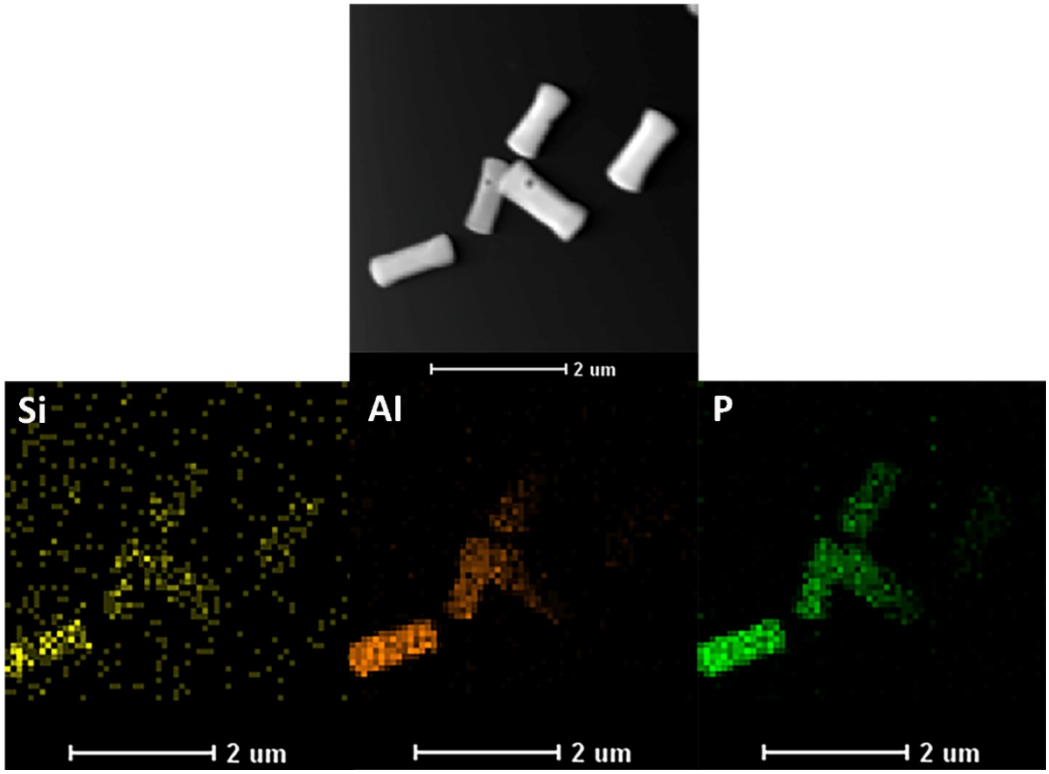

Fig. S2 Energy dispersion spectrometer (EDS) mapping of SAPO-17-S-1.

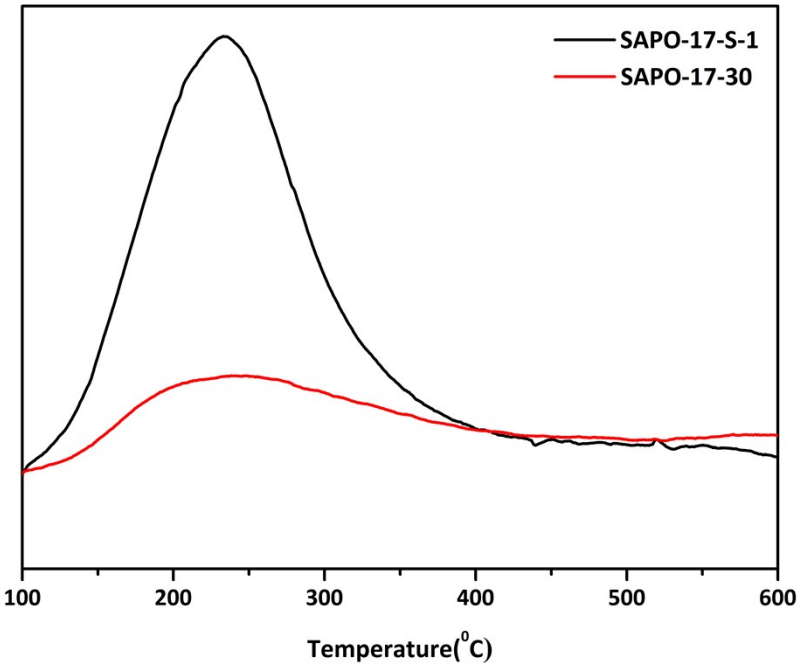

Fig. S3 Ammonium temperature-programmed desorption (NH_3-TPD) profile of synthesized SAPO-17-S-1 and SAPO-17-30.

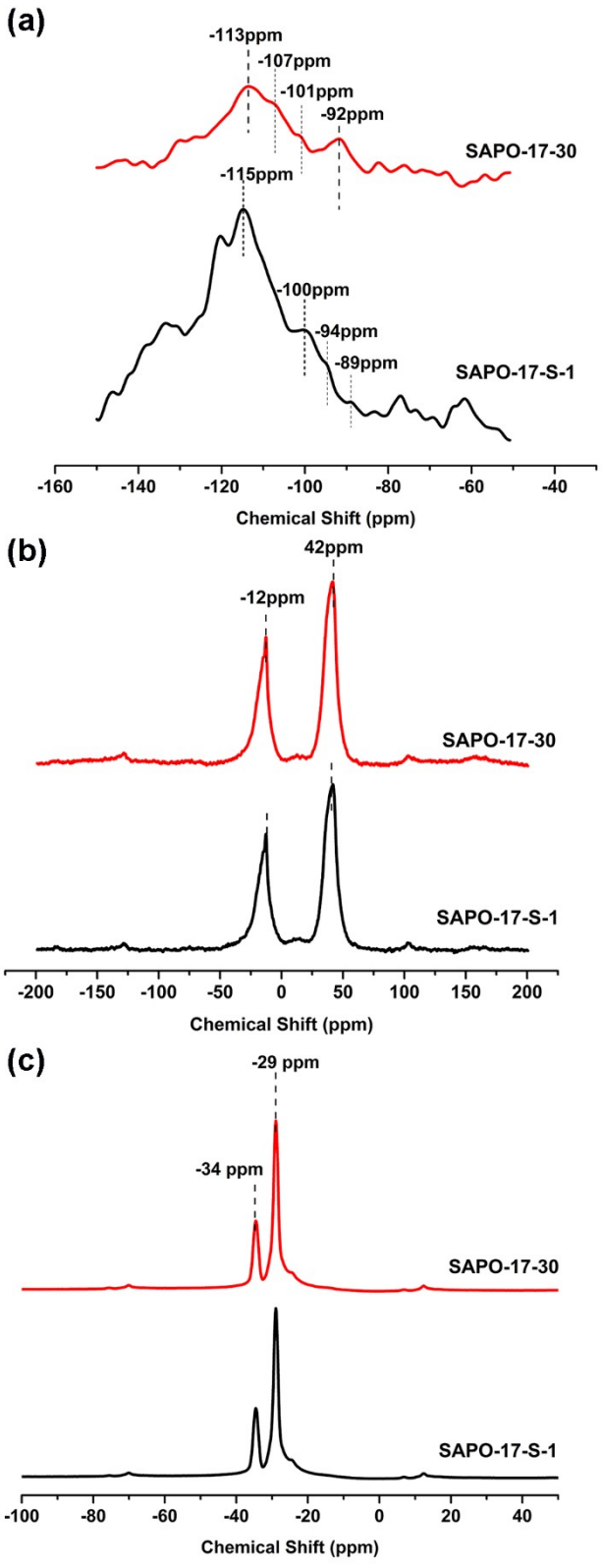

Fig. S4 ^{29}Si MAS NMR spectra (a), ^{27}AI MAS NMR spectra (b) and ^{31}P MAS NMR spectra (c) of SAPO-17-S-1 and SAPO-17-30 samples.

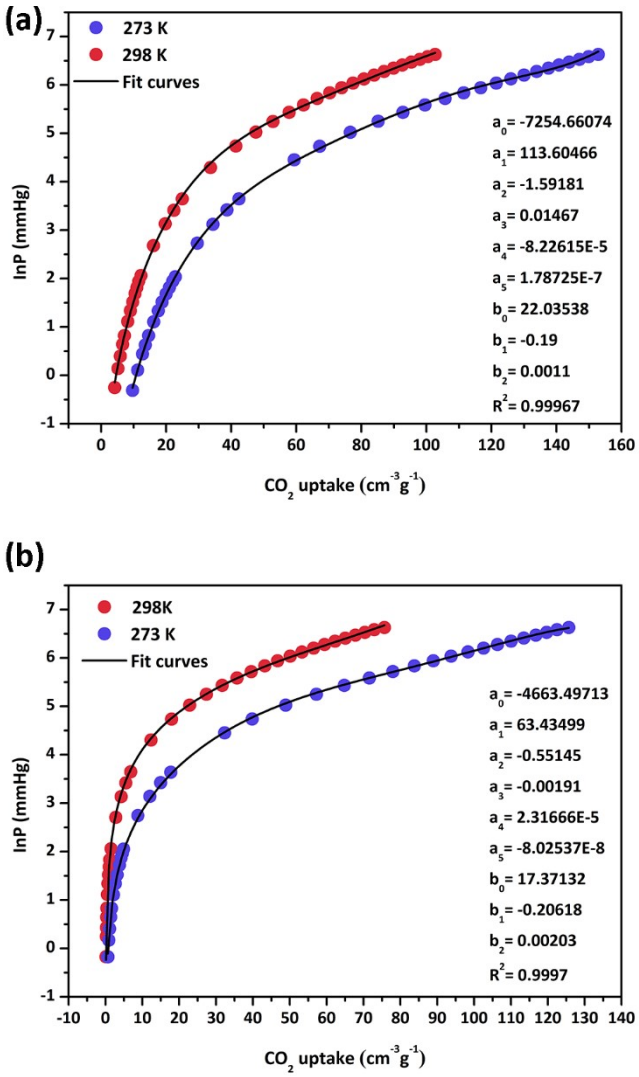

Fig. S5 Virial fitting for CO_2 of SAPO-17-S-1 (a) and SAPO-17-30 (b).

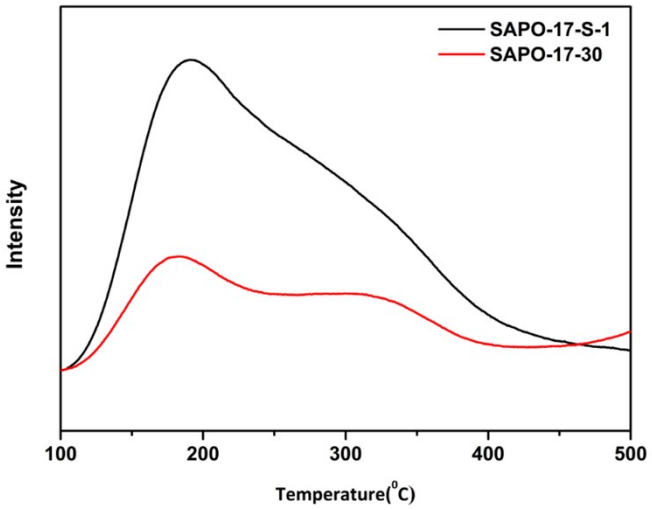

Fig. S6 CO_2-TPD profile of synthesized SAPO-17-S-1 and SAPO-17-30.

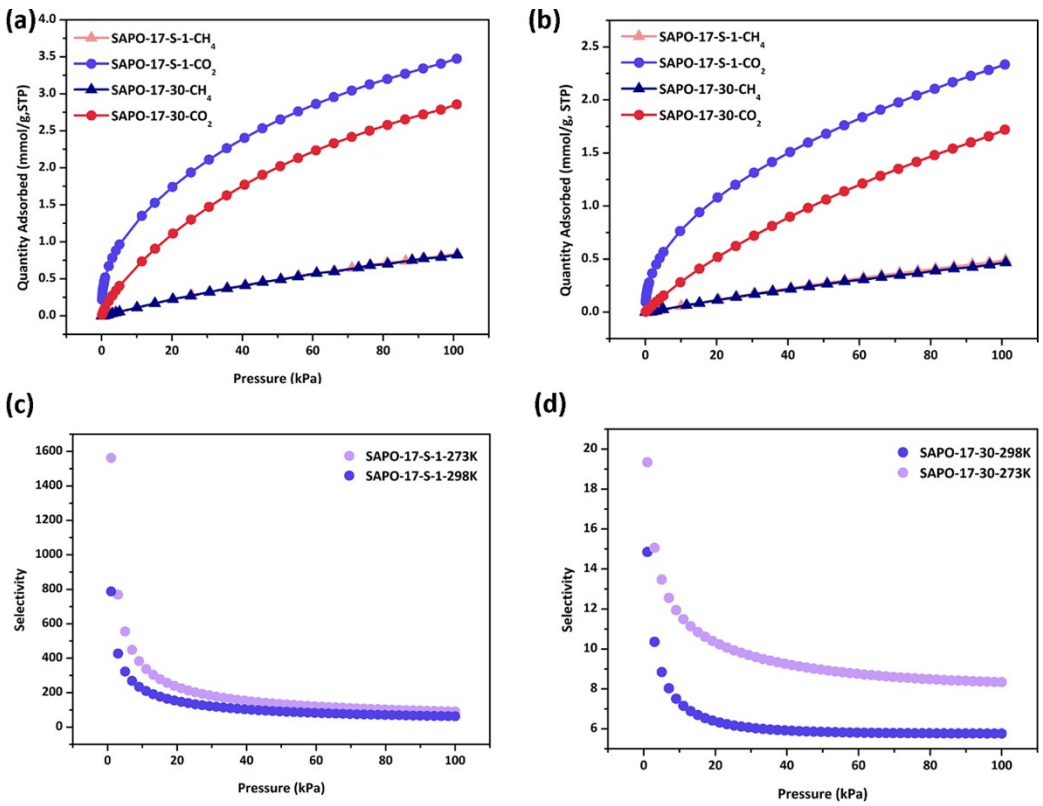

Fig. S7 CO_2, CH_4 adsorption-desorption isotherms of SAPO-17-S-1 and SAPO-17-30 at 273 K (a), 298 K (b), CO_2/CH_4 selectivity of SAPO-17-S-1 (c), SAPO-17-30 (d) at 273 K,298 K.

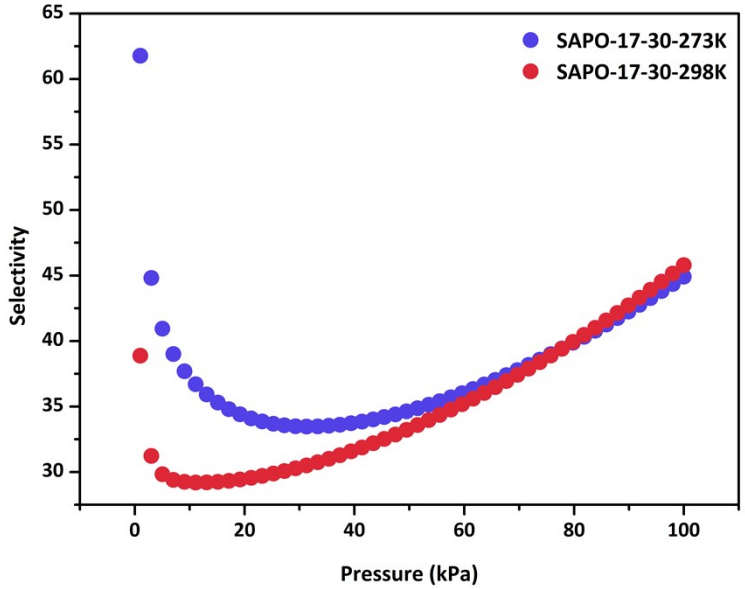

Fig. S8 CO_2/N_2 IAST selectivity of SAPO-17-30 at 273 K and 298 K.

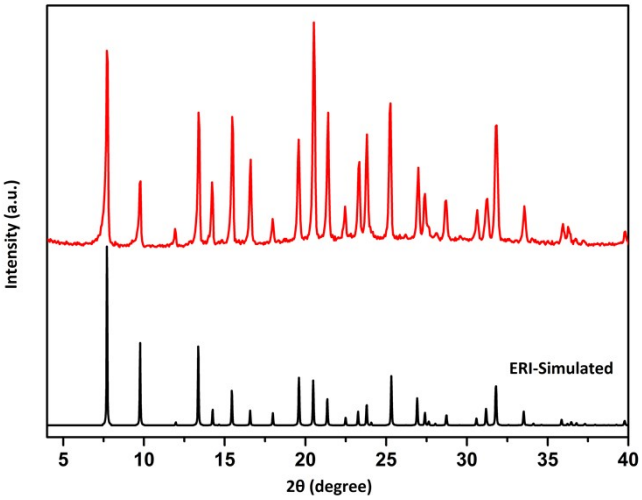

Fig. S9 XRD patterns of sample SAPO-17-S-1 after granulation.

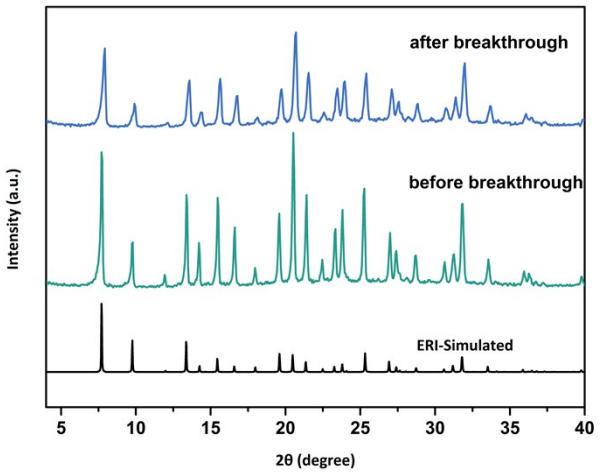

Fig. S10 XRD patterns of SAPO-17-S-1 before and after breakthrough experiments.

Table S1 The textural properties of SAPO-17-30, SAPO-17-180 and SAPO-17-S-1.

Sample	Si/(Si+Al+P)	S_{BET} [a] /(m^2/g)	S_{micro} [b] /(m^2/g)	S_{ext} [b] /(m^2/g)	V_{micro} [b] /(cm^3/g)	V_{total} [c] /(cm^3/g)
SAPO-17-30	0.038	511	478	33	0.23	0.24
SAPO-17-180	0.037	524	482	42	0.23	0.25
SAPO-17-S-1	0.04	594	547	47	0.26	0.29

[a] S_{BET} was calculated by BET equation from the linear part of adsorption isotherm ($0.05 < P / P_0 < 0.30$).

[b] S_{micro}, S_{ext} and V_{micro} are calculated by t-plot method.

[c] V_{total} is calculated at a pressure of $P / P_0 = 0.95$

Table S2 The fitting parameters of Dual-site Langmuir Freundlich formula for SAPO-17-S-1 at 273 K, 298 K.

Temperature	**273 K**		**298 K**	
Gas	**CO_2**	**N_2**	**CO_2**	**N_2**
q_{m1}	0.96244	0.07031	0.17109	0.04089
b_1	0.00269	0.0177	1.63771	0.00981
$1/C_1$	1.54446	1.4077	0.57532	1.62833
q_{m2}	67.31991	1.19658	16.13895	0.63961
b_2	0.00768	6.45822E-4	0.01051	4.51902E-4
$1/C_2$	0.36935	1.3493	0.58388	1.39483
R^2	1	0.9999	1	0.99989

Table S3 The fitting parameters of Dual-site Langmuir Freundlich formula for SAPO-17-30 at 273 K and 298 K.

Temperature	**273 K**		**298 K**	
Gas	**CO_2**	**N_2**	**CO_2**	**N_2**
q_{m1}	4.72844	0.0501	0.42672	0.0129
b_1	0.0113	0.00817	0.03616	0.0235
$1/C_1$	1.02373	1.96655	0.99566	1.60555
q_{m2}	0.20216	0.565	5.50477	0.27067
b_2	0.39487	4.36652E-4	0.00314	8.66997E-4
$1/C_2$	0.99644	1.61631	1.01147	1.37659
R^2	0.99999	0.99972	0.99999	0.99973

Table S4 Comparisons of CO_2 uptake and selectivity for the separation of CO_2/N_2, CO_2/CH_4 on various zeolites and SAPOs.

Material	Condition	CO_2 uptake (mmol/g)	CH_4 uptake (mmol/g)	N_2 uptake (mmol/g)	*S* (CO_2/CH_4)	*S* (CO_2/N_2)	Ref.
SAPO-17-S-1[a]	273 K, 101 kPa	3.47	0.83	0.36	91 (0.02/0.98 bar)	280 (0.15/0.85 bar)	This work
SAPO-17-30[a]	273 K, 101 kPa	2.86	0.82	0.29	5 (0.02/0.98 bar)	44 (0.15/0.85 bar)	This work
SAPO-56[b]	273 K, 101 kPa	5.5	—	0.52	—	10.5	1
SAPO-17[b]	273 K, 101 kPa	3.3	—	0.38	—	8.68	1
SAPO-35_0.14[a]	273 K, 101 kPa	4.8	—	0.45	—	40.4 (0.2/0.8 bar)	2
SAPO-17	298 K, 100 kPa	1.7	0.53	—	—	—	3
SAPO-43[c]	298 K, 100 kPa	1.07	0.16	0.07	—	15.28	4
SAPO-34	298 K, 100 kPa	2.26	0.4	—	5.7 (0.02/0.98 bar)	—	5
SAPO-DNL-6	298 K, 100 kPa	4.65	0.38	—	—	—	6
SAPO-RHO[a]	298 K, 100 kPa	4.41	0.83	0.23	26 (0.02/0.98 bar)	50 (0.15/0.85 bar)	7
Na-SAPO-RHO[a]	298 K, 100 kPa	3.5	≈0	0.09	2196 (0.02/0.98 bar)	196 (0.15/0.85 bar)	7
K-SAPO-RHO[a]	298 K, 100 kPa	0.9	≈0	≈0	—	29 (0.15/0.85 bar)	7
Cs-SAPO-RHO[a]	298 K, 100 kPa	0.5	≈0	≈0	—	22 (0.15/0.85 bar)	7
H-SSZ-13[a]	298 K, 100 kPa	3.98	0.22	—	—	73.6 (0.15/0.75 bar)	8
Cu-SSZ-13[a]	298 K, 100 kPa	3.75	0.25	—	—	72 (0.15/0.75 bar)	8
Fe-MOR[a]	273 K, 100 kPa	3.89	0.013	0.013	7.7×10^{123} (0.5/0.5 bar)	7.8×10^{41} (0.15/0.85 bar)	9
13X[a]	298 K, 100 kPa	5	0.26	0.22	103 (0.5/0.5 bar)	420 (0.1/0.9 bar)	10
Mg-MOF-74[a]	298 K, 100 kPa	8.00	1.11	—	137 (0.5/0.5 bar)	—	10
MIL-53(Al)[a]	298 K, 100 kPa	2.23	0.87	0.17	7 (0.1/0.9 bar)	22.8 (0.15/0.85 bar)	11
Li-ZK-5[d]	303K,	4.7	—	—		94	12

	100kPa						
Na-ZK-5 [d]	303K, 100kPa	4.0	—	—		56	12
K-ZK-5 [d]	303K, 100kPa	4.0	—	—		96	12
Mg-ZK-5 [d]	303K, 100kPa	4.4	—	—		121	12
Ca-ZK-5 [d]	303K, 100kPa	4.0	—	—		69	12
Na-MER[a]	298 K, 100 kPa	3.8	0.32		229 (0.02/0.98 bar)		13
K-MER[a]	298 K, 100 kPa	3.57	0.052		1818 (0.02/0.98 bar)		13

[a] IAST

[b] Relative ratio 1/1

[c] Single-component ratios 1/1

[d] $\alpha_{CO_2/N_2} = (\frac{N_{CO_2}}{N_{N_2}})/(\frac{y_{N_2}}{Y_{CO_2}})$

References

1. Cheung, Q. Liu, Z. Bacsik and N. Hedin, Silicoaluminophosphates as CO_2 sorbents, *Microporous Mesoporous Mater.*, 2012, **156**, 90−96.
2. Y. Li, H. Chen, C. Wang, Y. Ye, L. Li, X. Song and J. Yu, Achieving highly selective CO_2 adsorption on SAPO-35 zeolites by template-modulating the framework silicon content, *Chem. Sci.*, 2022, **13**, 5687−5692.
3. S. Zhong, N. Bu, R. Zhou, W. Jin, M. Yu and S. Li, Aluminophosphate-17 and silicoaluminophosphate-17 membranes for CO_2 separations, *J. Membr. Sci.*, 2016, **520**, 507−514.
4. J. Herna´ndez-Maldonado and R. T. Yang, Partially calcined gismondine type silicoaluminophosphate SAPO-43: Isopropylamine elimination and separation of carbon dioxide, hydrogen sulfide, and water, *Langmuir*, 2003, **19**, 2193−2200.
5. R. N. Salehi, S. Sharifnia and F. Rahimpour, Natural gas upgrading by selective separation on zeotype adsorbents, *J. Nat. Gas Sci. Eng.*, 2018, **54**, 37−46.
6. X. Su, P. Tian, D. Fan, Q. Xia, Y. Yang, S. Xu, L. Zhang, Y. Zhang, D. Wang and Z. Liu, Synthesis of DNL-6 with a high concentration of Si (4Al) environments and its application in CO_2 separation, *ChemSusChem*, 2013, **6**, 911−918.
7. X. Wang, N. Yan, M. Xie, P. Liu, P. Bai, H. Su, B. Wang, Y. Wang, L. Li, T. Cheng, P. Guo, W. Yan and J. Yu, The inorganic cation-tailored "trapdoor" effect of silicoaluminophosphate zeolite for highly selective CO_2 separatio, *Chem. Sci.*, 2021, **12**, 8803−8810.
8. M. R. Hudson, W. L. Queen, J. A. Mason, D. W. Fickel, R. F. Lobo and C. M. Brown, Unconventional, highly selective CO_2 adsorption in zeolite SSZ-13, *J. Am. Chem. Soc.*, 2012, **134**, 1970−1973.
9. Y. Zhou, J. Zhang, L. Wang, X. Cui, X. Liu, S. S. Wong, H. An, N. Yan, J. Xie, C. Yu, P. Zhang, Y. Du, S. Xi, L. Zheng, X. Cao, Y. Wu, Y. Wang, C. Wang, H. Wen, L. Chen, H. Xing and J. Wang, Self-assembled iron-containing mordenite monolithfor carbon dioxide sieving, *Science*, 2021, **373**, 315–320.
10. P. Nugent, Y. Belmabkhout, S. D Burd, A. J Cairns, R. Luebke, K. Forrest, T. Pham, S. Ma, B. Space, L. Wojtas, M. Eddaoudi and M. J. Zaworotko, Porous materials with optimal adsorption thermodynamics and kinetics for CO_2 separation, *Nature*, 2013, **495**, 80−84.
11. S. Kavak, H. M. Polat, H. Kulak, S. Keskin and A. Uzun, MIL-53(Al) as a versatile

platform for ionic-liquid/MOF composites to enhance CO_2 selectivity over CH_4 and N_2, *Chem. Asian J.*, 2019, **14**, 3655−3667.

12. Q. Liu, T. Pham, M. D. Porosoff and R. F. Lobo, ZK-5: A CO_2-selective zeolite with high working capacity at ambient temperature and pressure, *ChemSusChem*, 2012, **5**, 2237–2242.
13. V. M. Georgieva, E. L. Bruce, M. C. Verbraeken, A. R. Scott, W. J. Casteel, S. Brandani and P. A. Wright, Triggered gate opening and breathing effects during selective CO_2 adsorption by merlinoite zeolite, *J. Am. Chem. Soc.*, 2019, **141**, 12744–12759.